J Electr Eng Technol Vol. 8, No. 6: 1474-1480, 2013
http://dx.doi.org/10.5370/JEET.2013.8.6.1474

ISSN(Print) 1975-0102
ISSN(Online) 2093-7423

Effects of SPS Mold on the Properties of Sintered and Simulated SiC-ZrB_2 Composites

Jung-Hoon Lee*, In-Yong Kim*, Myeong-Kyun Kang*, Jun-Soo Jeon*, Seung-Hoon Lee*, An-Gyun Jeon* and Yong-Deok Shin†

Abstract – Silicon carbide (SiC)-zirconium diboride (ZrB_2) composites were prepared by subjecting a 60:40 vol% mixture of β-SiC powder and ZrB_2 matrix to spark plasma sintering (SPS) in 15 mmΦ and 20 mmΦ molds. The 15 mmΦ and 20 mmΦ compacts were sintered for 60 sec at 1500 °C under a uniaxial pressure of 50 MPa and argon atmosphere. Similar composites were simulated using Flux® 3D computer simulation software. The current and power densities of the specimen sections of the simulated SiC-ZrB_2 composites were higher than those of the mold sections of the 15 mmΦ and 20 mmΦ mold simulated specimens. Toward the centers of the specimen sections, the current densities in the simulated SiC-ZrB_2 composites increased. The power density patterns of the specimen sections of the simulated SiC-ZrB_2 composites were nearly identical to their current density patterns. The current densities of the 15 mmΦ mold of the simulated SiC-ZrB_2 composites were higher than those of the 20 mmΦ mold in the center of the specimen section. The volume electrical resistivity of the simulated SiC-ZrB_2 composite was about 7.72 times lower than those of the graphite mold and the punch section. The power density, 1.4604 GW/m^3, of the 15 mmΦ mold of the simulated SiC-ZrB_2 composite was higher than that of the 20 mmΦ mold, 1.3832 GW/m^3. The ZrB_2 distributions in the 20 mmΦ mold in the sintered SiC-ZrB_2 composites were more uniform than those of the 15 mmΦ mold on the basis of energy-dispersive spectroscopy (EDS) mapping. The volume electrical resistivity of the 20 mmΦ mold of the sintered SiC-ZrB_2 composite, 6.17×10^{-4} Ω cm, was lower than that of the 15 mmΦ mold, 9.37×10^{-4} Ω ·cm, at room temperature.

Keywords: Spark plasma sintering (SPS), Mold, Silicon carbide (SiC), Zirconium diboride (ZrB_2), Current density, Power density, Energy-dispersive spectroscopy (EDS), Flexural strength, Volume electrical resistivity, Simulated SiC-ZrB_2 composite, Sintered SiC-ZrB_2 composite

1. Introduction

The field-assisted sintering technique (FAST) and pulsed electric current sintering (PECS) belong to a class of novel sintering methods that employs a pulsed direct current (DC) to enhance consolidation, in order to produce sintered parts from metallic/ceramic powders. In the last decade, several variants of FAST/PECS techniques have been developed.

One example is spark plasma sintering (SPS), which is quite practical and may be applicable in various industries to reduce the thermal stresses of joints if suitable technological parameters are adopted. In particular, to better exemplify the advantages of this technique, it is simple and convenient to design various graded material interlayers in order to improve the compatibility of different materials and to reduce the thermal stresses of each layer.

The SPS technique has been used to fabricate various materials, including metals and alloys, compounds, ceramics, composites, bulk amorphous and nanomaterials, multi-scaled structures, and functionally graded materials [1, 2]. SPS is known as a single-step processing technique, which combines the electric field sintering technique and the uniaxial pressing forming technique. Some important technological benefits of SPS, such as higher heating rates, fewer processing steps, elimination of the need for sintering aids, and near net shape capacity, facilitate the control of grain growth and improve the mechanical, chemical, and physical properties of power materials [3].

The electrical resistivity of SiC is considered to be a negative temperature coefficient of resistance (NTCR) below 1000 °C. This causes increases in temperature and uncontrollable electrical current in SiC [4], resulting in overheating. However, the addition of SiC to ZrB_2 results in the formation of a SiC-ZrB_2 composite with high electrical conductivity, superior oxidation resistance, and high mechanical strength. These properties make SiC-ZrB_2 composites suitable conductive materials and Ohmic-

† Corresponding Author: Department of Electrical Engineering, Wonkwang University, Korea. (ydshin@ wonkwang.ac.kr)
* Department of Electrical Engineering, Wonkwang University, Korea. (ljh0820@hanmail.net)
Received: March 27, 2013; Accepted: June 5, 2013

contact electrode materials, able to function satisfactorily at both high and low temperatures [5-7].

The dispersion of ZrB_2 or other metal borides in SiC-based matrices was found to be useful in the production of materials for heaters and igniters on the basis of their adequate resistivities, positive temperature coefficients of resistance (PTCR), greater strength and toughness compared to matrix SiC, and good oxidation resistance at temperatures up to approximately 1200 °C [8].

This study was performed to determine whether the current and power densities of a simulated SiC-ZrB_2 composite correlated with the experimentally measured properties of sintered SiC-ZrB_2 composites according to the mold size used during SPS.

The densification, mechanical, and electrical properties of the sintered SiC-ZrB_2 composites were evaluated by conducting apparent density and flexural strength measurements, high resolution x-ray diffraction (HR-XRD) and field-emission scanning electron microscopy (FE-SEM) studies, energy-dispersive spectroscopy (EDS) mapping, and volume electrical resistivity measurements. The current and power densities of a simulated SiC-ZrB_2 composite were analyzed using Flux® 3D computer simulation software.

2. Experimental Procedure

2.1 Powder preparation

High-purity β-SiC (Grade BF12, H. C. Starck, Germany) and ZrB_2 (Grade B, H. C. Starck, Germany) were combined in a 60:40 vol% ratio. The measured materials were mixed with distilled water in a polyurethane bowl (volume: 1583.4 mL). The mixture was then subjected to planetary ball mill processing with high-purity SiC balls (a 1:5 mixture of 10 mmΦ and 20 mmΦ diameter SiC balls) for 24 h. Next, the powders were dehydrated by heating for 12 h at 100 °C, and sieved through a 60-mesh screen.

2.2 Sintering process

The dried powders were respectively placed in a graphite die with an inner diameter of 15 mmΦ or 20 mmΦ, enclosed with graphite foil, and sintered using a PAS-H3000 apparatus (ElTek Co., Ltd, Korea) at a sintering temperature of 1500 °C and uniaxial pressure of 50 MPa under argon atmosphere. The sintered composites and the simulated SiC-ZrB_2 composites were classified according to the diameter of the mold (15 mmΦ and 20 mmΦ).

2.3 Physical characteristics

Theoretical densities of the sintered SiC-ZrB_2 composites were calculated on the basis of the rule of mixtures (3.217 g/cm^3 for β-SiC and 6.085 g/cm^3 for ZrB_2).

The final sintered SiC-ZrB_2 composites were ground with a diamond wheel and shaped into disks. Then, the relative density of each of the sintered composite specimens was measured 10 times by the Archimedes method.

The disks were machined to obtain sintered SiC-ZrB_2 composite bars with dimensions of 1.0×0.7×10 mm^3. The bars were polished using 1 μm diamond paste and beveled at 45° for mechanical testing (ASTM F394-78).

The three-point flexural strength of each sintered compact was measured approximately 5-6 times at room temperature using a material testing apparatus (Model 4204, Instron, USA) under the following conditions: outer span, 10 mm; inner span, 8 mm; and crosshead speed, 0.07 mm/min.

The microstructures of the fracture surfaces of the flexural strength test specimens were observed using FE-SEM (S-4800, Hitachi, Japan). EDS mapping (S-4800, Horiba, Japan) was carried out to analyze the atom distribution in the sintered SiC-ZrB_2 composites. The sintered SiC-ZrB_2 compacts were cut by wire electrical discharge machining (WEDM, α-OPiB, FANAC, Japan) to produce specimens for volume electrical resistivity measurements. The volume electrical resistivity of each specimen processed by WEDM was measured 200 times by the van der Pauw method [9].

2.4 Computer simulation

The Flux® 3D (CEDRAT, France) computer software package was used to analyze the effect of the SPS mold size on the electric field of the simulated SiC-ZrB_2 composites. Details of the simulations for the SiC-ZrB_2 composites follow in Sections 2.4.1 and 2.4.2, for the computer-simulated SiC-ZrB_2 composite. The electric field of the simulated SiC-ZrB_2 composite was analyzed by applying Flux® 3D computer software [10].

2.4.1 Geometric designs of the SPS molds

The area sections for the quantitative analysis of the current and power densities of the simulated SiC-ZrB_2 composites are designated by horizontal and vertical dotted lines, respectively, as shown in Fig. 1. The horizontal specimen sections of the 15 mmΦ and 20 mmΦ molds were 7.5-22.5 mm and 5-25 mm, respectively. The horizontal mold sections for the 15 mmΦ mold were 0-7.5 mm and 22.5-30 mm; those of the 20 mmΦ mold were 0-5 mm and 25-30 mm, as shown Fig. 1. The vertical punch sections of the 15 mmΦ specimen were 27.5-47.5 mm and 52.5-72.5 mm, and those of the 20 mmΦ specimen were 25.5-47.5 mm and 52.5-74.5 mm. The vertical specimen sections of the 15 mmΦ and the 20 mmΦ molds were 47.5-52.5 mm, as shown in Fig. 1.

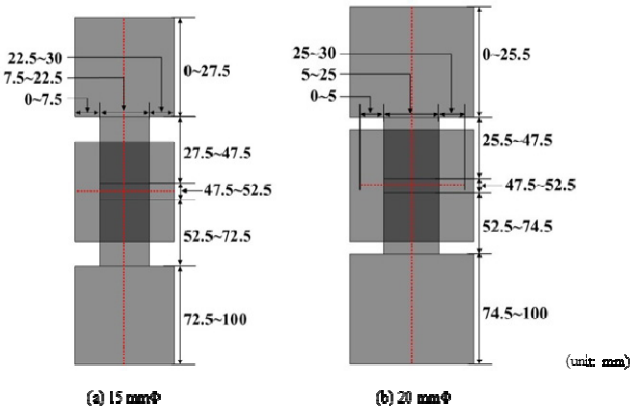

Fig. 1. Geometric designs of the SPS molds

2.4.2 Parameters for Computer Simulation

The input parameters of the physical properties for the computer simulation of the simulated SiC-ZrB_2 composites were the applied voltage, the volume electrical resistivity, and the relative permittivity. The applied voltage was DC 5 V; the volume electrical resistivity was the average value (7.77×10^{-4} Ω·cm) [11] of the volume electrical resistivities of the sintered SiC-ZrB_2 composites; and the relative permittivity of the sintered SiC-ZrB_2 composite was obtained by applying following equation.

relative permittivity of a SiC-ZrB_2 composite

$$= \frac{\varepsilon_{\text{sic}} \times \varepsilon_{ZrB_2}}{\left(\varepsilon_{\text{sic}} \times \theta_{ZrB_2}\right) + \left(\varepsilon_{ZrB_2} \times \theta_{\text{sic}}\right)} \quad (1)$$

where, ε_{SiC_2}, the relative permittivity of SiC, and ε_{ZrB_2}, the relative permittivity of ZrB_2, were 10.0455 and 0.5498, respectively [12]. θ_{SiC_2}, the volume percentage of SiC, and θ_{ZrB_2}, the volume percentage of ZrB_2, were 60 vol% and 40 vol%, respectively.

3. Experimental Results and Discussion

3.1 Computer-simulated current and power densities

Fig. 2 shows the vertical cross sections for the quantitative analyses of the current densities of the simulated SiC-ZrB_2 composites. The arrows indicate the flow of current density and the colors of the arrows reflect the intensity of the current density. In Fig. 2, it can be seen that the current densities were the highest in the specimen sections of the simulated SiC-ZrB_2 composites. The volume electrical resistivity of the SiC-ZrB_2 composite, 7.77×10^{-4} Ω·cm, was found to be lower than that (6.0×10^{-3} Ω·cm) of the graphite mold. Fig. 2 also shows that the current density by Joule heating due to thermal conduction and convection phenomena was higher in the punch section of the graphite mold than elsewhere.

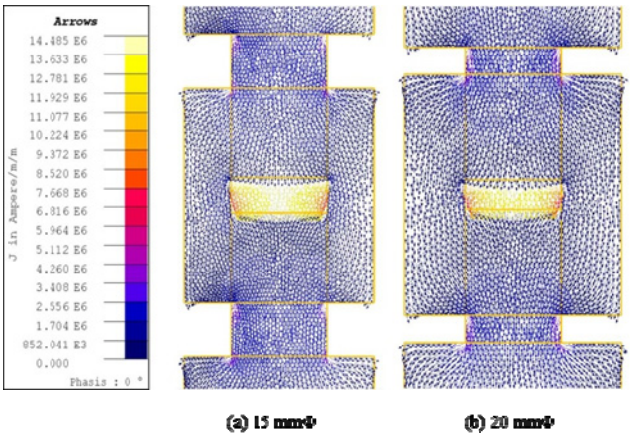

Fig. 2. Current density distributions of the vertical cross sections of the graphite molds

Although the conditions for SPS were the same, the sintering properties of the simulated SiC-ZrB_2 composites were different according to mold size. The Joule heating in the punch section of the graphite mold is produced by itself, and that of the specimen section of the SiC-ZrB_2 composite is produced by itself and spark plasma phenomena [13-15]. The distribution section of the current density between the graphite mold and the specimen in the simulated SiC-ZrB_2 composite was different because of differing resistances.

Figs. 3 and 4 show the horizontal and vertical specimen sections for the quantitative analyses of the current densities of the simulated SiC-ZrB_2 composites. In these figures, the specimen section current densities were higher than those of the 15 mmΦ and 20 mmΦ mold sections. With a closer approach to the center of the horizontal specimen section, the current densities of the simulated SiC-ZrB_2 composites grew larger, as shown in Fig. 3. Also, the current density of the 15 mmΦ mold of the simulated SiC-ZrB_2 composite was higher than that of the 20 mmΦ mold in the center of the specimen section (Fig. 3). Thus, the volume electrical resistivity of the simulated SiC-ZrB_2 composite was about 7.72 times lower than that of the graphite mold and punch. Also, the flow of current density in the simulated SiC-ZrB_2 composite was confirmed to be concentrated in the 15 mmΦ mold.

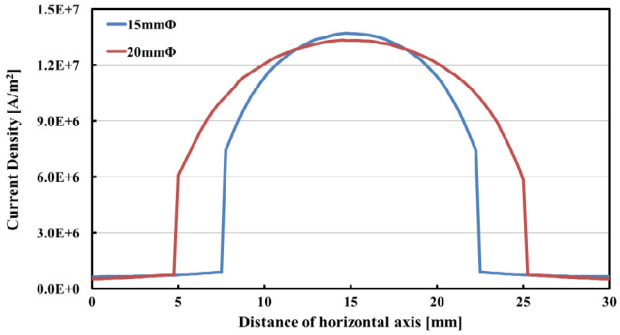

Fig. 3. Current densities in horizontal sections of 15 mmΦ and 20 mmΦ specimens

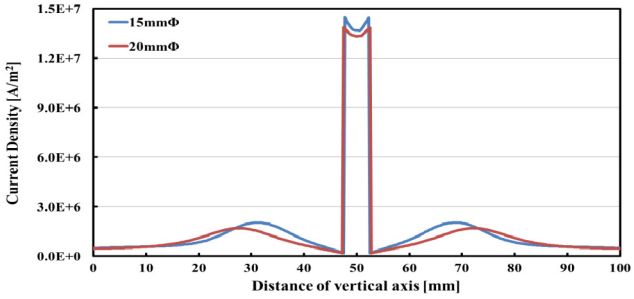

Fig. 4. Current densities in vertical sections of 15 mmΦ and 20 mmΦ specimens

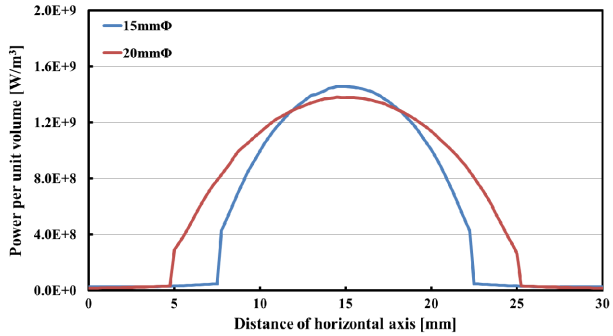

Fig. 5. Power densities in horizontal sections of 15 mmΦ and 20 mmΦ specimens

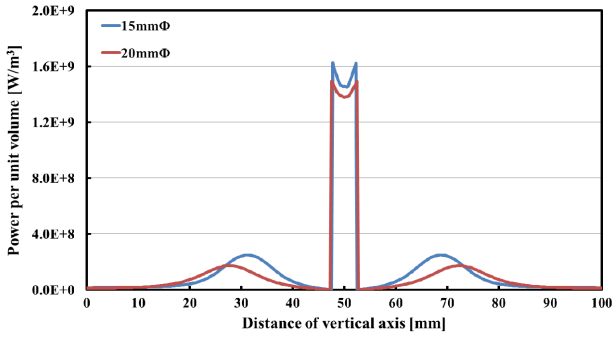

Fig. 6. Power densities in vertical sections of 15 mmΦ and 20 mmΦ specimens

Figs. 5 and 6 show the horizontal and vertical specimen sections for the quantitative analyses of the power densities of the simulated SiC-ZrB_2 composites. The power density patterns of the simulated composite specimen sections were nearly identical to those of the current density patterns. Fig. 5 reveals that the power density, 1.4604 GW/m^3, of the 15 mmΦ mold of the simulated SiC-ZrB_2 composite was higher than that of the 20 mmΦ mold (1.3832 GW/m^3) in the center of horizontal specimen section.

3.2 Properties of the sintered SiC-ZrB_2 composites

As shown in Table 1, the flexural strength of the 20 mmΦ mold of the sintered SiC-ZrB_2 composites was lower than that of the 15 mmΦ mold at a sintering temperature of 1500 °C and uniaxial pressure of 50 MPa under argon atmosphere. The flexural strength of a sintered SiC-ZrB_2 composite is dependent on its relative density. It was confirmed that varying the SPS mold size affected the properties of the sintered and simulated SiC-ZrB_2 composites. The HR-XRD analyses of the sintered SiC-ZrB_2 composites are shown in Fig. 7. All the peak values appeared on International Centre for Diffraction Data (ICDD) cards, with the following code numbers: 00-029-1128 (SiC), 01-074-1302 (SiC), 00-042-1091 (SiC), and 01-075-0964 (ZrB_2). No evidence of reaction between β-

Table 1. Properties of the sintered SiC-ZrB_2 composites [11]

Properties / Mold	Relative Density (%)	Flexural Strength (MPa)	Volume Electrical Resistivity (× 10^{-4} Ω·cm)	XRD
15 mmΦ	99.40	1011.34	9.37	SiC, ZrB_2
20 mmΦ	97.88	392.30	6.17	SiC, ZrB_2

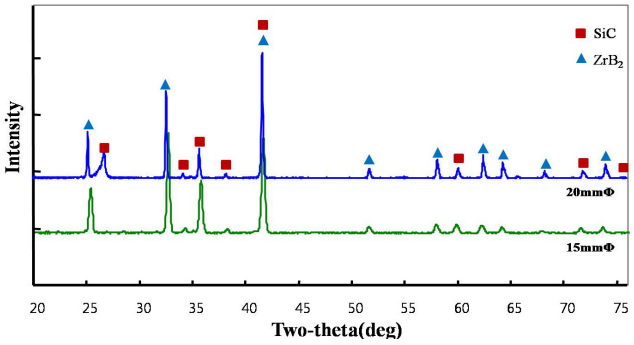

Fig. 7. High-resolution x-ray diffraction patterns of the sintered SiC-ZrB_2 composites

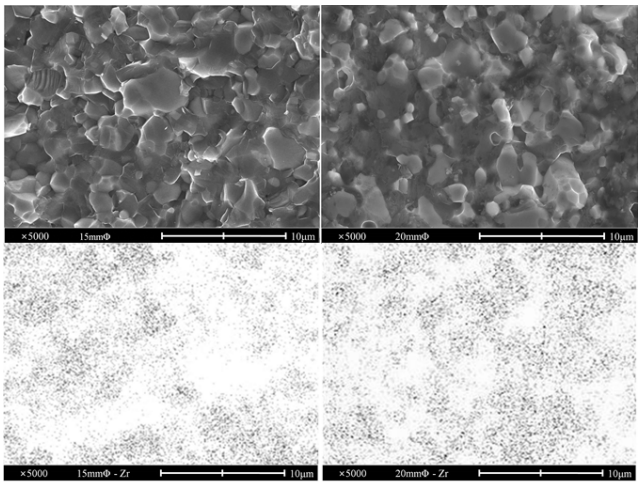

(a) 15 mmΦ (b) 20 mmΦ

Fig. 8. Field-emission scanning electron microscopy and energy-dispersive spectroscopy mapping of the sintered SiC-ZrB_2 composites

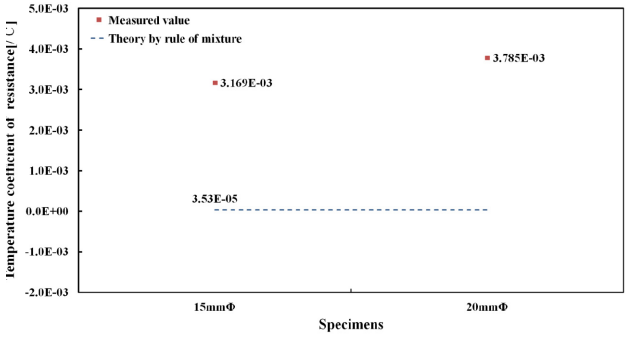

Fig. 9. Temperature coefficient of resistance of the sintered SiC-ZrB_2 composites

SiC and ZrB_2 in the sintered SiC-ZrB_2 composites under argon atmosphere was observed in the HR-XRD analysis.

Fig. 8 shows that the ZrB_2 distribution in the 20 mmΦ mold of the sintered SiC-ZrB_2 composite was more uniform than that of the 15 mmΦ mold on the basis of EDS mapping. Table 1 revealed that the volume electrical resistivity of the 15 mmΦ mold specimen was higher than that of the 20 mmΦ mold at room temperature, because the ZrB_2 chain formations were broken by the frequent occurrence of spark plasmas in the 15 mmΦ molded specimen. Thus, the experimental values of the volume electrical resistivities of the sintered SiC-ZrB_2 composites were dependent on the ZrB_2 distribution, because electrical current flows predominantly by the ZrB_2 chain formations with their low electrical resistivities. This also explains why the current and power densities of the 15 mmΦ mold of the simulated SiC-ZrB_2 composites were higher than those of the 20 mmΦ mold in the center of the specimen section, as the ZrB_2 chain formations are broken by the frequent occurrence of spark plasmas in the 15 mmΦ mold of the sintered SiC-ZrB_2 composites.

Fig. 9 shows the temperature coefficient of resistance (TCR) of the sintered SiC-ZrB_2 composites, calculated to be 3.53×10^{-5}/°C using the rule of mixtures, and the experimental values, which were measured by the van der Pauw method [8, 16]. The TCRs of the 15 mmΦ and 20 mmΦ molds were 3.169×10^{-3}/°C and 3.785×10^{-3}/°C, respectively, indicating that all the sintered SiC-ZrB_2 composites had a PTCR. The 15 mmΦ mold had a lower PTCR than the 20 mmΦ mold because chain formations of ZrB_2 in the 15 mmΦ mold of the sintered SiC-ZrB_2 composite were broken by the frequent occurrence of spark plasmas under the high applied pulse voltage.

4. Conclusion

Sintered SiC-ZrB_2 composites were produced according to mold size at a sintering temperature of 1500 °C and uniaxial pressure of 50 MPa under argon atmosphere by subjecting a 60:40 vol% mixture of β-SiC powder and ZrB_2 matrix to spark plasma sintering. The current and power densities of the simulated SiC-ZrB_2 composites according to mold size were calculated using the Flux® 3D computer simulation software. The following results were obtained:

1. The current densities of the specimen sections of the simulated SiC-ZrB_2 composites were higher than those of the mold sections in both the 15 mmΦ and the 20 mmΦ molds. Toward the centers of the horizontal specimen sections, the current densities of the simulated SiC-ZrB_2 composites became large.
2. The power density patterns of the specimen sections of the simulated SiC-ZrB_2 composites were nearly identical to those of the current density patterns.
3. The power density, 1.4604 GW/m^3, of the 15 mmΦ mold of the simulated SiC-ZrB_2 composite was higher than that of the 20 mmΦ mold, 1.3832 GW/m^3, in the center of the horizontal specimen section.
4. No evidence of reaction between β-SiC and ZrB_2 in the sintered SiC-ZrB_2 composites under argon atmosphere was observed in the HR-XRD analysis.
5. The ZrB_2 distributions in the 20 mmΦ mold of the sintered SiC-ZrB_2 composites were more uniform than those of the 15 mmΦ mold on the basis of EDS mapping.
6. The volume electrical resistivity of the 20 mmΦ mold of the sintered SiC-ZrB_2 composite was lower than that of the 15 mmΦ mold at room temperature, because the ZrB_2 chain formations were broken by the frequent occurrence of spark plasmas in the 15 mmΦ mold.

The current densities of the specimen sections of the simulated SiC-ZrB_2 composites were the highest. The volume electrical resistivity of SiC-ZrB_2 composite, 7.77×10^{-4} Ω·cm, was lower than that of the graphite mold (6.0×10^{-3} Ω·cm). The current density of the punch section of the graphite mold was higher than those of the others. It is considered that current density by Joule heating due to the phenomenon of thermal conduction and convection was higher in the punch section than those of the others.

Finally, the current and power densities of the 15 mmΦ mold of the simulated SiC-ZrB_2 composites were higher than those of the 20 mmΦ mold in the center of the specimen section, as the chain formations of ZrB_2 were broken by the frequent occurrences of spark plasmas in the 15 mmΦ mold of the sintered SiC-ZrB_2 composite.

Acknowledgements

This paper was supported by wonkwang university in 2013.

References

[1] D. M. Bi, W. Zhi and W. G. Qin, "Exploration of joining between ceramics and steels: An example

using the spark plasma sintering technique," *J. Phase Equilib. Diffus.* 32[3], 2011.
[2] D. Tiwari, B. Basu and K. Biswas, "Simulation of thermal and electric field evolution during spark plasma sintering," *Ceram. Int.,* 35, pp. 699-708, 2009.
[3] Y. Song, Y. Li, Z. Zhou, Y. Lai and Y. Ye, "A multi-field coupled FEM model for one-step-forming process of spark plasma sintering considering local densification of powder material," *J. Mater*. Sci., 46, pp. 5645-5656, 2011.
[4] H. Hashiguchi and H. Kimugasa, "Electrical resistivity of α-SiC ceramics added with NiO," *J. Ceram. Soc. Japan,* 102[2], pp. 160-64, 1994.
[5] J. Y. Ju, Ch. H. Kim, J. J. Kim, J. H. Lee, H. S. Lee and Y. D. Shin, "The development of an electro-conductive SiC-ZrB_2 ceramic heater through spark plasma sintering," *J. Elec. Eng. & Tech*., 4[4], pp. 538-545, 2009.
[6] J. H. Lee, J. Y. Ju, Ch. H. Kim, J. H. Park, H. S. Lee and Y. D. Shin, "The development of an electroconductive SiC-ZrB_2 composite through spark plasma sintering under argon atmosphere," *J. Elec. Eng. & Tech.*, 5[2], pp. 342-351, 2010.
[7] J. H. Lee, J. Y. Ju, Ch. H. Kim and Y. D. Shin, "A study on optimum spark plasma sintering conditions for conductive SiC-ZrB_2 composites," *J. Elec. Eng. & Tech.,* 6[4], pp. 543-550, 2011.
[8] D. Sciti, C. Melandri and A. Bellosi, "Properties of ZrB_2-reinforced ternary composites," *Adv. Eng. Mater.,* 6[9], pp. 775-781, 2004.
[9] L. J. van der Pauw, "A method of measuring specific resistivity and Hall effect of disc of arbitrary shapes," *Philips Res. Repts,* 13[1], pp. 1-9, 1958.
[10] CEDRAT, "FLUX® 10 User's guide," 2009. Ref.: K101-10-EN-06/09.
[11] Y. D. Shin, J. H. Lee, J. Y. Park, J. Y. Ju and H. S. Lee, "Effects of mold on properties of SiC-ZrB_2 composites through SPS," *Proc. of the 42nd KIEE Summer Conf.* 2011, pp. 1515-1516, 2011.
[12] http://www.matweb.com
[13] X. Song, X. Liu and J. Zhang, "Neck Formation and self-adjusting mechanism of neck growth of conducting powders in spark plasma sintering," *J. Am. Ceram. Soc.,* 89[2], pp. 494-500, 2006.
[14] Y. D. Shin, J. H. Lee, B. S. Jin and H. S. Kim, "The electrical field analysis of SiC-ZrB_2 composites through SPS," *High Voltage and Discharge Application Engineering Society of KIEE*, pp. 53-54, 2011.
[15] U. Anselmi-Tamburini, S. Gennari, J. E. Garay and Z. A. Munir, "Fundamental investigations on the spark plasma sintering/synthesis process," *Mater. Sci. Eng.,* A394, pp. 139-148, 2005.
[16] Y. D. Shin, J. Y. Ju and J. S. Kwon, "Electrical conductive mechanism of hot-pressed α-SiC-ZrB_2 composites," *Trans. KIEE*, 48C[2], pp. 104-108, 1999.

Jung-Hoon Lee He was born in Korea in 1983. He received his B.S. and M.S. degrees in Electrical Engineering from Wonkwang University, Iksan, Korea, in 2008 and 2010, respectively. Presently, he is pursuing a Ph.D. degree at Wonkwang University.

In-Yong Kim He was born in Korea in 1969. He received his B.S. and M.S. degrees in Electrical Engineering from Wonkwang University, Iksan, Korea, in 1995 and 2011, respectively. Presently, he is pursuing a Ph.D. degree at Wonkwang University. Korea Institute of Nuclear Safety, department of instrumentation Control & Electricity

Myeong-Kyun Kang He was born in Korea in 1987. He received B.S. degree in Electrical Engineering from Wonkwang University, Iksan, Korea, in 2012. Presently, he is pursuing a M.S. degree at Wonkwang University.

Jun-Soo Jeon He was born in Korea in 1986. He received B.S. degree in Electrical Engineering from Wonkwang University, Iksan, Korea, in 2012. Presently, he is pursuing a M.S. degree at Wonkwang University.

Seung-Hoon Lee He was born in Korea in 1988. He received B.S. degree in Electrical Engineering from Wonkwang University, Iksan, Korea, in 2013. Presently, he is pursuing a M.S. degree at Wonkwang University.

An-Gyun Jeon He was born in Korea in 1961. He received his M.S. degree in the Department of Electrical Engineering, Chonbuk National University, Jeonju, Korea in 1996. He is currently a Ph.D course in the Department of Electrical Engineering, Wonkwang Uni-

versity, Iksan, Korea. He is currently a Professor in the Dept. of Eletrical Engineering, Honam University, Gwangju, Korea.

Yong-Deok Shin He was born in Korea in 1953. He received his B.S. degree in Electrical Engineering from Wonkwang University, Iksan, Korea, in 1983, where he worked as a research assistant and part-time lecturer from 1983 to 1988. He worked at the Center Research Institute of Keyang Electric Machinery Co., Ltd/from 1988 to 1990. He received his ph. D. degree from Sungkyunkwan University, Seoul, Korea, in 1991. He was a visiting Professor at Pennsylvania State University, Pennsylvania, USA, in 1998 and 2005. Currently, he is a professor of the Department of Electrical Engineering at Wonkwang University, Iksan, Korea and a fellow member of the Korean Institute of Electrical Engineers (KIEE)